Available online at www.sciencedirect.com
SCIENCE DIRECT
Journal of Molecular Catalysis A: Chemical 242 (2005) 218–223
JOURNAL OF MOLECULAR CATALYSIS A: CHEMICAL
www.elsevier.com/locate/molcata

New catalysts for dichlorodifluoromethane hydrolysis: Mesostructured titanium and aluminum phosphates

Jie Zhao, Bozhi Tian, Yinghong Yue, Weiming Hua *, Dongyuan Zhao *, Zi Gao

Department of Chemistry and Shanghai Key Laboratory of Molecular Catalysis and Innovative Materials, Fudan University, Shanghai 200433, PR China

Received 29 April 2005; accepted 31 May 2005
Available online 12 September 2005

Abstract

Catalytic decomposition of CCl_2F_2 in the presence of water vapor and air was investigated over mesoporous titanium and aluminum phosphates. They are much more active than the ordinary titanium and aluminum phosphates. Comparison between two mesoporous catalysts shows that mesoporous aluminum phosphate is slightly more active than mesoporous titanium phosphate, but the latter catalyst exhibits higher stability than the former one during the reaction. The results based on NH_3-TPD and IR show that the activity of the catalysts is correlated with their surface acidity and hydroxyl groups.

Keywords: CCl_2F_2 hydrolysis; Solid acids; Mesoporous titanium phosphate; Mesoporous aluminum phosphate

1. Introduction

Chlorofluorocarbons (CFCs) diffused into the stratosphere deplete the ozone layer and they are greenhouse gases too [1,2]. Various kinds of CFCs have been banned since the Montreal Protocol signed in 1987. However, there are still 2.25 million-tonnes of CFCs all over the world and numerous air-conditioning systems are still using them as coolants. If these CFCs are released to the environment without pretreatment, they will still endanger the ozone layer in the future. Several methods to destroy CFCs have been developed so far. Among them catalytic hydrolysis appears to be the most practical and promising approach because of the simple process, readily available water, high conversion and mild reaction conditions [3,4]. Many types of acid catalysts, such as zeolites [5], heteropolyacids [6], alumina-based catalysts [7,8], titania- or zirconia-based catalysts [9–14] and metal phosphates [4,15–18], have been attempted for the hydrolysis of CFCs.

Since the pioneering work of the Mobil researchers in the development of silica mesoporous molecular sieves in 1992 [19], mesoporous inorganic materials have attracted increasing interest because of high surface area, large pore volume and uniform mesopores, which provide potential applications as catalysts or catalyst supports involving bulky molecules. Thermally stable mesoporous metal phosphates have been successfully synthesized in several groups [20–24] using the supramolecular assembly approach developed by researchers at Mobil. More recently, block copolymer templating synthesis of ordered stable mesoporous metal phosphates based on an acid–base pair route was developed in our university [25,26]. However, so far there have been no reports describing the use of mesoporous metal phosphates as catalysts for the hydrolysis of CFCs.

In this work, mesoporous titanium and aluminum phosphates were synthesized based on an acid–base pair route. The catalytic hydrolysis of CCl_2F_2 over these materials has been investigated and compared with ordinary metal phosphates.

* Corresponding authors. Tel.: +86 2165642409; fax: +86 2165641740.
E-mail address: wmhua@fudan.edu.cn (W. Hua).

1381-1169/$ – see front matter © 2005 Elsevier B.V. All rights reserved.
doi:10.1016/j.molcata.2005.05.039

2. Experimental

2.1. Preparation of catalysts

Mesoporous aluminum and titanium phosphates were synthesized following the procedure in the literature [25,26]. 5 mmol $AlCl_3$, 5 mmol H_3PO_4 and 0.1 mmol F127 were added to 0.65 mol ethanol. The mixture was stirred vigorously for 30 min at room temperature and transferred into a dish to evaporate ethanol at 40 °C for 6 h then at 80 °C for additional 2 h. The product obtained was calcined at 550 °C for 6 h in air. Mesoporous aluminum phosphate is designated as m-AlPO. Mesoporous titanium phosphate (labeled as m-TiPO) was prepared in the similar way by using $Ti(OC_4H_9)_4$–PCl_3 as an acid–base pair and triblock copolymer P123 as a structure-directing agent. The ordinary aluminum phosphate (designated as AlPO) was synthesized by a precipitation method [27]. 0.25 M aqueous NH_3 solution was added dropwise to an aqueous solution composed of stoichiometric amounts of aluminum nitrate and 85 wt.% H_3PO_4 under stirring until pH 4.5, and then aged for 24 h. The precipitate was filtered, washed thoroughly with deionized water, dried at 110 °C for 24 h and finally calcined at 550 °C for 6 h. The ordinary titanium phosphate (designated as TiPO) was prepared by mixing aqueous $Ti(SO_4)_2$ solution and 85 wt.% H_3PO_4 under stirring. The precipitate obtained was treated in the same manner as the above.

2.2. Catalyst characterization

The wide-angle XRD patterns were recorded on a Rigaku D/MAX-IIA diffractometer using Cu Kα radiation, whereas the small angle XRD patterns were recorded on a Bruker D4 ENDEAVOR diffractomater using Cu Kα radiation. The N_2 adsorption/desorption isotherms were measured on a Micromeritics ASAP 2000 instrument at −196 °C. The specific surface areas of the samples were calculated from the adsorption isotherms by the BET method, and pore size distributions from the adsorption isotherms by the BJH method. Transmission electron microscopy (TEM) was conducted on a JEOL-2011 instrument. The temperature-programmed desorption of NH_3 (NH_3-TPD) of the samples was carried out in a flow-type fixed-bed reactor. The NH_3 adsorption temperature was 120 °C, and the temperature was raised at a rate of 10 °C min^{-1}. The desorbed NH_3 was collected in a liquid N_2 trap and analyzed by gas chromatography. For infrared spectroscopic (IR) study, self-supporting wafers with a density of ca. 3 mg cm^{-2} of the catalysts were prepared. IR spectrum was recorded on a Perkin-Elmer 983G spectrometer after evacuation at 300 °C for 3 h.

2.3. Reaction testing

The catalytic hydrolysis of CCl_2F_2 was carried out in a continuous fixed-bed flow microreactor under atmospheric pressure. CCl_2F_2 (1000 ppm), water vapor (6000 ppm) and balance air were mixed and passed through 0.4 g catalyst (40–60 mesh) at a flow rate of 40 ml min^{-1}. Effluent gases were passed through a KOH solution to eliminate HF and HCl produced during the reaction. Unreacted CCl_2F_2 and another possible $CClF_3$ by-product were separated with an Apiezon grease L/SiO_2 column at 70 °C and then analyzed by gas chromatography. The experimental data were obtained at 1 h after reaching the desired temperature by sequential heating, unless otherwise stated.

3. Results and discussion

3.1. Structural characterization

The wide-angle XRD patterns of mesoporous titanium and aluminum phosphates as well as the phosphates of Ti and Al are shown in Fig. 1. Only a very diffuse reflection near $2\theta = 25°$ was observed in the scan range of 10–80°, indicating that these samples are amorphous. Fig. 2 shows the small-angle XRD patterns of mesoporous metal phosphates. The m-AlPO sample exhibits an intense reflection at 0.69° and a very weak peak at 1.36°, whereas the m-TiPO sample displays a

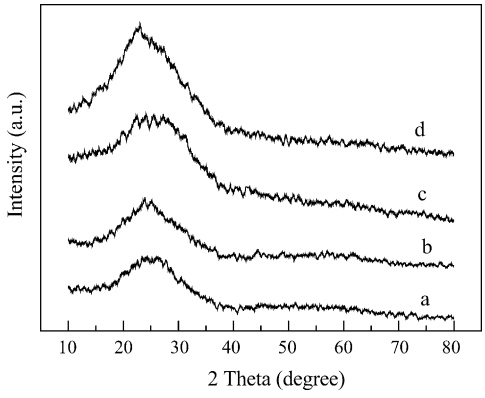

Fig. 1. XRD patterns of the samples in the wide-angle region. (a) m-TiPO; (b) TiPO; (c) m-AlPO and (d) AlPO.

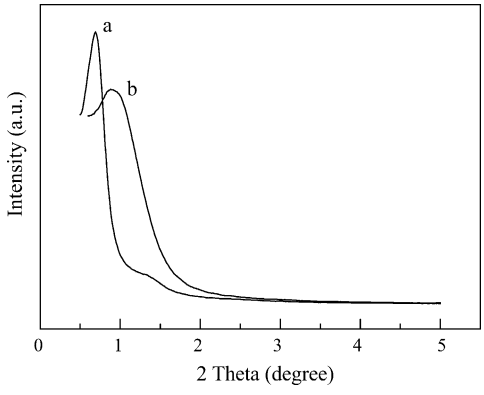

Fig. 2. XRD patterns of (a) m-AlPO and (b) m-TiPO in the small-angle region.

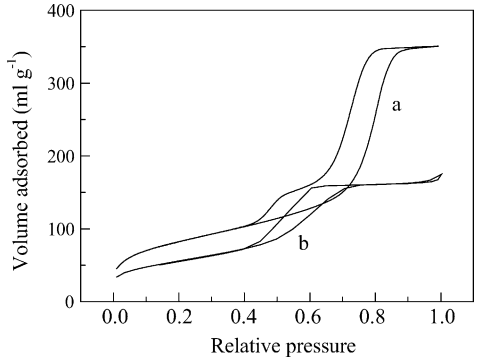

Fig. 3. N_2 adsorption/desorption isotherms of (a) m-AlPO and (b) m-TiPO at −196 °C.

single reflection at 0.88°. The diffraction peaks in the small angle region are assigned to mesostructure.

Fig. 3 illustrates the N_2 adsorption/desorption isotherms of mesoporous titanium and aluminum phosphates. The BJH pore size distributions of the samples are presented in Fig. 4. The isotherms for both samples are of type IV with a typical H1 hysteresis loop at high relative pressure, which is related to the capillary condensation in the mesoporous channels. The m-AlPO sample exhibits a much larger hysteresis loop than m-TiPO, and the hysteresis loop appears in the P/P_0 range of 0.44–0.91 for m-AlPO and 0.43–0.72 for m-TiPO, suggesting that the pore volume and pore diameter of the former sample are higher than those of the latter one. A narrow pore size distribution centered at 10.2 nm for the m-AlPO sample and at 4.8 nm for m-TiPO is observed, as revealed in Fig. 4. The BJH pore size distributions of the AlPO and TiPO samples are shown in Fig. 5. Both samples exhibit a rather broad pore size distribution, and the pores in these samples are those of the aggregates of nanosized nonporous particles.

The specific surface area, pore volume and the most probable pore diameter of all the samples are summarized in Table 1. It is clear that the surface areas of mesoporous metal phosphates are much higher than those of the respective metal phosphates. The pore volume of m-AlPO is larger than that of AlPO. However, the pore volume of m-TiPO is smaller than that of TiPO, which is due to the wider pore diameter of the

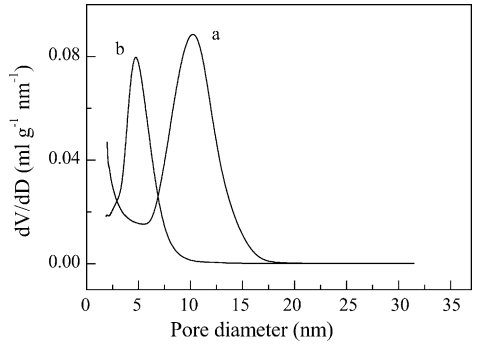

Fig. 4. Pore size distributions of (a) m-AlPO and (b) m-TiPO.

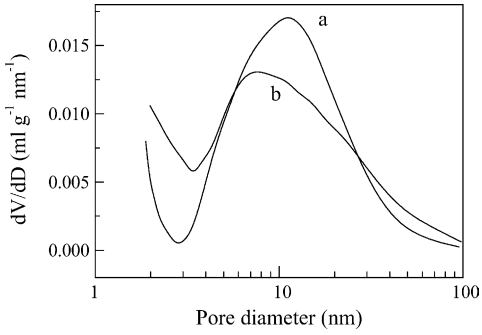

Fig. 5. Pore size distributions of (a) AlPO and (b) TiPO.

Table 1
Textural properties of the samples

Sample	Surface area ($m^2\ g^{-1}$)	Pore diameter (nm)	Pore volume ($cm^3\ g^{-1}$)
m-TiPO	201.9	4.8	0.26
TiPO	122.6	7.5	0.40
m-AlPO	298.6	10.2	0.54
AlPO	139.7	10.9	0.41

latter sample. Comparison between both mesoporous metal phosphates shows that the m-AlPO sample has higher specific surface area, larger pore volume and wider pore diameter than m-TiPO. The TEM images of m-TiPO and m-AlPO are given in Fig. 6. The worm-like channels are observed for both samples.

3.2. Acidic properties of the samples

The surface acidity of the samples was measured by NH_3-TPD method. There is only one broad peak on the NH_3-TPD profiles of all the samples, as shown in Fig. 7. The peak temperature and number of acid sites on the samples are summarized in Table 2. The peak temperatures are in the range of 227–324 °C, showing that the acid sites of the samples are of weak-medium strength. The acid strength and number of acid sites of the m-TiPO sample are greater than those of TiPO. The acid strength of m-AlPO is identical to that of AlPO, and the number of acid sites on the former sample is lower than that on the latter one. The Ti-containing samples possess stronger acid sites than the Al-containing ones.

Table 2
Results of NH_3-TPD and the CCl_2F_2 hydrolysis reaction

Catalyst	NH_3–TPD		CCl_2F_2 hydrolysis	
	Peak temperature (°C)	NH_3 desorbed (mmol g^{-1})	T_{50} (°C)	T_{90} (°C)
m-TiPO	324	0.586	400	455
TiPO	297	0.503	420	475
m-AlPO	227	1.066	400	445
AlPO	226	1.362	505	560

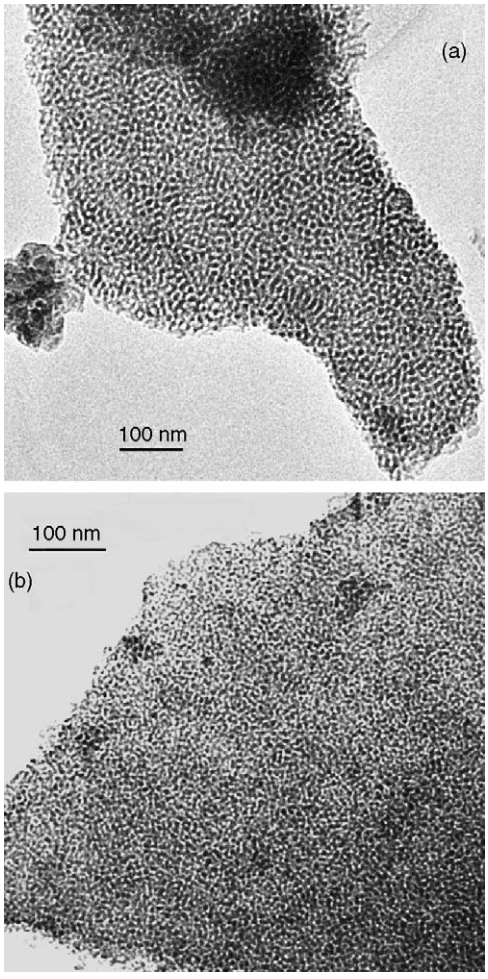

Fig. 6. TEM images of (a) m-AlPO and (b) m-TiPO.

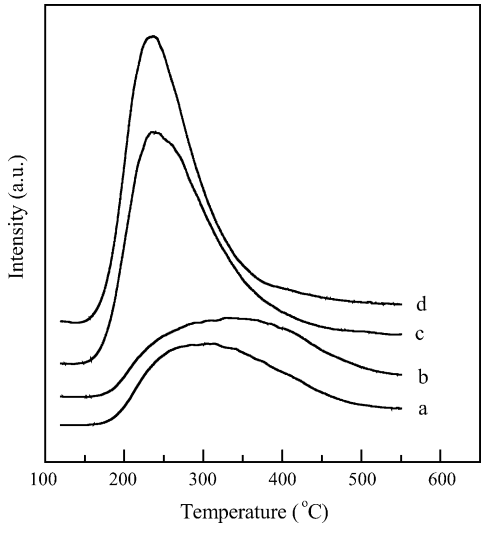

Fig. 7. NH_3-TPD profiles of (a) TiPO, (b) m-TiPO, (c) m-AlPO and (d) AlPO.

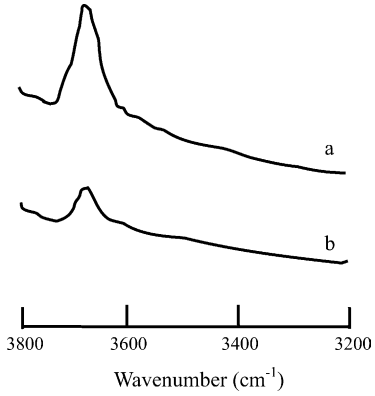

Fig. 8. IR spectra of (a) m-AlPO and (b) AlPO.

3.3. IR spectroscopy

The infrared adsorptions of the hydroxyl groups on m-AlPO and AlPO were measured after evacuation at 300 °C and depicted in Fig. 8. The spectra of the two samples are similar, presenting a band in the 3800–3200 cm^{-1} region at 3669 cm^{-1} corresponding to the hydroxyl group vibration. It is evident that the relative intensity of the hydroxyl group vibration of m-AlPO is higher than that of AlPO, indicating that the former sample is more abundant in hydroxyl groups.

3.4. Catalytic hydrolysis of CCl_2F_2

The activities of the catalysts for the hydrolysis of CCl_2F_2 were tested and depicted in Fig. 9 as a function of reaction temperature. Their activities increase with reaction temperature. The temperatures at which 50 and 90% of CCl_2F_2 were converted (designated as T_{50} and T_{90}, respectively) were read from the curves and used as a measure of the decomposition activities. The T_{50} and T_{90} of the m-AlPO catalyst are 400 and 445 °C, respectively, which are ca. 100 °C lower than those of the AlPO catalyst (see Table 2). This indicates that the former catalyst is much more active than the latter one. The activity of the m-TiPO catalyst is also higher than that of TiPO. Comparison between two mesoporous catalysts shows that the m-AlPO catalyst is slightly more active than m-TiPO.

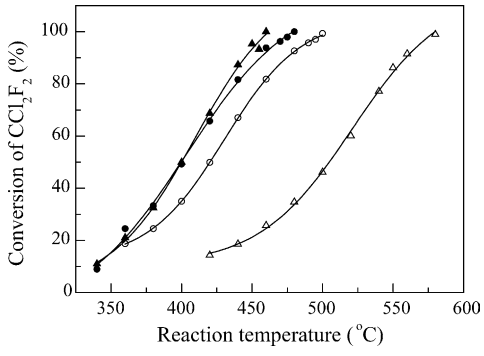

Fig. 9. CCl_2F_2 conversion on (●) m-TiPO, (◯) TiPO, (▲) m-AlPO and (△) AlPO as a function of reaction temperature.

Table 3
Selectivity to $CClF_3$ at different CCl_2F_2 conversions

Catalyst	Conversion (%)	$CClF_3$ selectivity (%)
m-TiPO	24.5	0.2
	96.3	0.5
TiPO	24.5	0.2
	95.7	0.5
m-AlPO	21.0	0.2
	95.4	5.7
AlPO	34.7	3.1
	91.6	8.2

The major reaction of CCl_2F_2 decomposition in the presence of water vapor and air is

$$CCl_2F_2 + 2H_2O \rightarrow CO_2 + 2HF + 2HCl$$

As recognized by many researchers, acid center is very important for the decomposition of CFCs [7–9,15,16]. Karmakar and Greene [9] suggested that the reaction proceeds through the following steps: adsorption of CCl_2F_2 molecules on Bronsted acid sites, the reaction between adsorbed CCl_2F_2 and neighboring surface hydroxyls to produce intermediates such as $COCl_2$ and COFCl, the reaction between these intermediates and water to form complete oxidation products. According to this mechanism, the surface acidity of the catalysts should play an important role in the reaction. Here, the surface acidity refers to the acid strength and acid number of the samples. Therefore, the higher activity of m-TiPO than TiPO is associated with the higher acidity of the former catalyst. The activity difference between two mesoporous phosphates can be also interpreted by their acidities. However, the surface acidity of m-AlPO is lower than that of AlPO, which does not coincide with their activities. According to the above reaction mechanism, surface hydroxyls could be also very important for the hydrolysis of CCl_2F_2. Hence, we consider that the higher activity of m-AlPO than AlPO is caused by the more hydroxyl groups on the former catalyst, as revealed by IR result. In this case, it does not mean that Bronsted acid sites on the catalyst are not involved in the reaction, but the surface hydroxyls are more important for the reaction.

$CClF_3$ may form as a major by-product in the CCl_2F_2 decomposition reaction. Table 3 shows the selectivity to $CClF_3$ at different CCl_2F_2 conversions. The amount of $CClF_3$ detected in the effluent did not exceed 0.5% on the Ti-containing phosphates. However, the selectivity to $CClF_3$ is much higher on the Al-containing phosphates, and it increases with the conversion of CCl_2F_2.

The catalyst life is an important factor for practical use. The catalytic stability of mesoporous titanium and aluminum phosphates was tested. To clarify the changes in activity with time, the test was carried out at 465 °C for m-TiPO and at 435 °C for m-AlPO because the conversion of CCl_2F_2 would not reach 100% under this condition. As illustrated in Fig. 10, the conversion decreases with time on stream during the initial 9 h and then it appears to keep steady within the test period. The decline in activity is greater for m-AlPO than for m-TiPO. In the whole reaction course of 100 h the selectivity to $CClF_3$ did not exceed 0.5% over m-TiPO. Interestingly, an increase in selectivity to $CClF_3$ was observed over m-AlPO in the initial 5 h. This observation is probably related to the surface fluorination of m-AlPO, since Takita et al. [16] proposed that $CClF_3$ is formed through halogen exchange between the F^- ions on the catalyst surface and the CCl_2F_2 molecules, i.e. $CCl_2F_2 + F^- \rightarrow CClF_3 + Cl^-$.

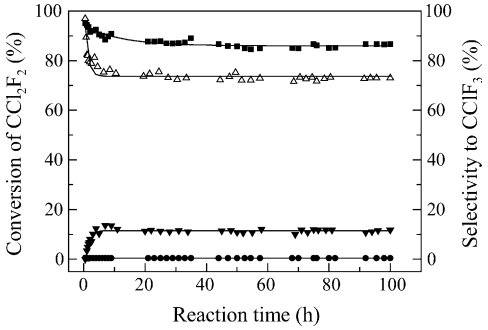

Fig. 10. Activity and selectivity of m-TiPO and m-AlPO during 100 h on stream. (■, ●) m-TiPO; (△, ▼) m-AlPO. (■, △) conversion of CCl_2F_2; (●, ▼) selectivity to $CClF_3$.

4. Conclusions

The hydrolysis of CCl_2F_2 in the presence of water vapor and air was studied over mesoporous metal phosphates. Mesoporous titanium phosphate (m-TiPO) is much more active than the ordinary titanium phosphate, which is related to the higher acidity of the former catalyst. The activity of mesoporous aluminum phosphate (m-AlPO) is obviously higher than that of the ordinary aluminum phosphate, which is associated with the more surface hydroxyl groups of the former catalyst. The activity of m-AlPO is slightly higher than that of m-TiPO, but the latter catalyst displays the higher catalytic stability.

Acknowledgements

This work was funded by the Chinese Major State Basic Research Development Program (2000077507), the Shanghai Major Basic Research Program (03DJ14004) and the National Natural Science Foundation of China (20303004).

References

[1] M.J. Molina, F.S. Rowland, Nature 249 (1974) 810.
[2] J.R. Hummel, R.A. Reck, Atmos. Environ. 15 (1982) 379.
[3] S. Okazaki, A. Kurosaki, Chem. Lett. (1989) 1901.
[4] Y. Takita, Shokubai 41 (1999) 284.
[5] M. Tajima, M. Niwa, Y. Fujii, Y. Koinuma, R. Aizawa, S. Kushiyama, S. Kobayashi, K. Mizuno, H. Ohuchi, Appl. Catal. B 9 (1996) 167.

[6] Z. Ma, W.M. Hua, Y. Tang, Z. Gao, Chin. J. Catal. 21 (2000) 3.
[7] H. Nagata, T. Takakura, S. Tashiro, M. Kishida, K. Mizuno, I. Tamori, K. Wakabayashi, Appl. Catal. B 5 (1994) 23.
[8] C.F. Ng, S. Shan, S.Y. Lai, Appl. Catal. B 16 (1998) 209.
[9] S. Karmakar, H.L. Greene, J. Catal. 151 (1995) 394.
[10] M. Tajima, M. Niwa, Y. Fujii, Y. Koinuma, R. Aizawa, S. Kushiyama, S. Kobayashi, K. Mizuno, H. Ohuchi, Appl. Catal. B 12 (1997) 263.
[11] X.Z. Fu, W.A. Zeltner, Q. Yang, M.A. Anderson, J. Catal. 168 (1997) 482.
[12] Z. Ma, W.M. Hua, Y. Tang, Z. Gao, Chin. J. Chem. 18 (2000) 341.
[13] Z. Ma, W.M. Hua, Y. Tang, Z. Gao, Chem. Lett. (1999) 1215.
[14] W.M. Hua, F. Zhang, Z. Ma, Y. Tang, Z. Gao, Catal. Lett. 65 (2000) 85.
[15] Y. Takita, G.L. Li, R. Matsuzaki, H. Wakamatsu, H. Nishiguchi, Y. Moro-oka, T. Ishihara, Chem. Lett. (1997) 13.
[16] Y. Takita, M. Ninomiya, R. Matsuzaki, H. Wakamatsu, H. Nishiguchi, T. Ishihara, Phys. Chem. Chem. Phys. 1 (1999) 2367.
[17] Y. Takita, H. Wakamatsu, G.L. Li, Y. Moro-oka, H. Nishiguchi, T. Ishihara, J. Mol. Catal. A 155 (2000) 111.
[18] Y. Takita, H. Wakamatsu, M. Tokumaru, H. Nishiguchi, M. Ito, T. Ishihara, Appl. Catal. A 194–195 (2000) 55.
[19] C.T. Kresge, M.E. Leonowicz, W.J. Roth, J.C. Vartuli, J.S. Beck, Nature 359 (1992) 710.
[20] D.Y. Zhao, Z.H. Luan, L. Kevan, Chem. Commun. (1997) 1009.
[21] J. Jimenez-Jimenez, P. Maireles-Torres, P. Olivera-Pastor, E. Rodriguez-Castellon, A. Jimenez-Lopez, D.J. Jones, J. Roziere, Adv. Mater. 10 (1998) 812.
[22] D.J. Jones, G. Aptel, M. Brandhorst, M. Jacquin, J. Jimenez-Jimenez, A. Jimenez-Lopez, P. Maireles-Torres, I. Piwonski, E. Rodriguez-Castellon, J. Zajac, J. Roziere, J. Mater. Chem. 10 (2000) 1957.
[23] T. Kimura, Y. Sugahara, K. Kuroda, Micropor. Mesopor. Mater. 22 (1998) 115.
[24] M. Tiemann, M. Schulz, C. Jager, M. Froba, Chem. Mater. 13 (2001) 2885.
[25] B.Z. Tian, X.Y. Liu, B. Tu, C.Z. Yu, J. Fan, L.M. Wang, S.H. Xie, G.D. Stucky, D.Y. Zhao, Nat. Mater. 2 (2003) 159.
[26] L.M. Wang, B.Z. Tian, J. Fan, X.Y. Liu, H.F. Yang, C.Z. Yu, B. Tu, D.Y. Zhao, Micropor. Mesopor. Mater. 67 (2004) 123.
[27] Y. Takita, C. Morita, M. Ninomiya, H. Wakamatsu, H. Nishiguchi, T. Ishihara, Chem. Lett. (1999) 417.